Available online at www.sciencedirect.com
ScienceDirect
Trans. Nonferrous Met. Soc. China 24(2014) 49−57
Transactions of Nonferrous Metals Society of China
www.tnmsc.cn

Dry sliding friction and wear behaviors of $Mg_2B_2O_5$ whisker reinforced 6061Al matrix composites

Pei-peng JIN, Geng CHEN, Li HAN, Jin-hui WANG

School of Mechanical Engineering, Qinghai University, Xining 810016, China

Received 29 October 2012; accepted 30 January 2013

Abstract: The friction and wear properties of $Mg_2B_2O_5$ whisker reinforced 6061Al matrix composite fabricated via power ultrasonic-stir casting process were investigated using a ball-on-disk wear-testing machine against a GCr45 steel counterface under dry sliding conditions. The reinforcements include as-received $Mg_2B_2O_5$ whiskers and $Mg_2B_2O_5$ whiskers coated with CuO and ZnO. The volume fraction of the composites is 2%. The relationship between the wear rate and the coefficient of friction was discussed. The results indicate that the wear rate of the $Mg_2B_2O_5$ whiskers coated with ZnO reinforced aluminum matrix composites is the lowest among the materials. As the applied load and sliding speed steadily increase the coefficients of friction and wear rates of the as-received matrix alloy and the fabricated composites decrease. As the applied load and sliding speed increase, the wear mechanisms of the composites shift from a mild to a severe regime.

Key words: metal-matrix composite; sliding wear; wear testing; wear mechanism

1 Introduction

Particle/whisker-reinforced metal-matrix composites (MMCs), particularly aluminum matrix composites, are known for their low density, high specific strength and specific stiffness. MMCs also have good resistance to abrasion, temperature, and impact, as well as good shock absorption, good dimensional stability and casting. These advantages contribute to the wide acceptance of aluminum matrix composites in high-technology structural and functional applications in fields such as aerospace, automotive, defense, electronic industries, sports and recreation [1−9]. Many researchers have made significant achievements on the friction and wear behaviors of aluminum matrix composites. Most of these achievements focus on the particle/fiber-reinforced aluminum-based matrix composites, such as SiC, $NiAl_3$, Al_2O_3 and B_4C [10−12]. However, few studies have investigated the sliding wear behavior of $Mg_2B_2O_5$ whisker-reinforced aluminum matrix composites. In addition, our recent experiment results showed that the tensile strength of the ZnO/$Mg_2B_2O_{5w}$/AZ31B composite is improved significantly compared with the $Mg_2B_2O_{5w}$/AZ31B composite [13]. Therefore, the friction and wear behaviors of whiskers coated with metal oxides reinforced composites remain unclear and deeper understanding on the wear mechanism of these composites is needed.

In this work, the friction and wear behaviors of $Mg_2B_2O_5$ whisker reinforced 6061Al-matrix composites under dry sliding were investigated. Three types of whiskers were used, namely, the as-received $Mg_2B_2O_5$ whisker, the $Mg_2B_2O_5$ whisker coated with CuO and $Mg_2B_2O_5$ whisker coated with ZnO.

2 Experimental

2.1 Materials

Power ultrasonic-stir casting process was used to fabricate the $Mg_2B_2O_5$ whiskers and CuO- and ZnO-coated $Mg_2B_2O_5$ whisker reinforced aluminum alloy composites (denoted as $Mg_2B_2O_{5w}$/6061Al, CuO/$Mg_2B_2O_{5w}$/6061Al and ZnO/$Mg_2B_2O_{5w}$/6061Al, respectively). The volume fractions of the whiskers in the three types of composites are 2%. The chemical composition of the 6061 aluminum alloy is shown in Table 1. The $Mg_2B_2O_5$ whisker is a type of single crystal.

Foundation item: Project (2011CB612200) supported by the National Basic Research Program of China
Corresponding author: Pei-peng JIN; Tel: +86-971-5363028; E-mail: jinpeipeng@hotmail.com
DOI: 10.1016/S1003-6326(14)63027-2

Table 1 Chemical composition of 6061Al alloy (mass fraction, %)

Al	Si	Fe	Cu
95.1−97.5	0.40−0.80	0.70	0.15−1.40
Mg	Mn	Cr	Zn
0.8−1.2	0.15	0.04−0.35	0.25−0.35

Although its properties are similar to those of the SiC whisker, the $Mg_2B_2O_5$ whisker only costs one-fiftieth of the SiC whisker. The aluminum alloys were heated first into melts in a stainless steel crucible. The temperature was kept at 700−750 °C. Upon formation of a vortex via mechanical stirring, the preheated whiskers were added to the melt. The molten composites were stirred for 1−5 min to force the whiskers mixing with the melt. The whiskers were then dispersed in the melt via power ultrasonication for 5 −10 min with continuous mechanical stirring. Both the stirrer and the power ultrasonicator were made from Ti alloy. Samples for wear-testing (60 mm in diameter, 10 mm in thickness) were prepared by pouring the melt into cylindrical-shaped sand moulds.

A schematic diagram of the power ultrasonic-stir casting is shown in Fig. 1.

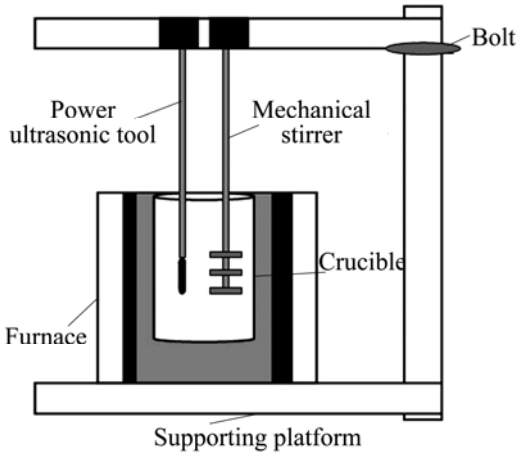

Fig. 1 Schematic diagram of power ultrasonic-stir casting

2.2 Wear test

The wear tests were conducted using a ball-on-disk wear-testing machine against a GCr45 steel counterface under loads of 5−25 N. The wear tests were conducted at a sliding velocity of 120−480 m/min with a constant sliding distance of 1 km at room temperature. Before and after the wear tests, the mass of the samples was obtained on an electronic balance with up to 0.1 mg of accuracy. Before the wear tests, all the specimens were polished using 1000# SiC water sandpaper. Both the ball and the samples were cleaned with acetone and dried before and after each test. The wear rate was calculated from the mass loss measurement.

After the wear tests, a scanning electron microscope (SEM) was used to observe the worn surface and debris of the specimens.

3 Results and discussion

3.1 Effect of whisker surface treatment on wear behaviors of composites

Figures 2(a)−(d) show the friction coefficient curves of the different materials at an applied load of 15 N and a sliding velocity of 480 m/min. It can be seen that the friction and wear processes of the matrix alloy and the composites consist of two stages. The first stage is the running-in period, at which the friction coefficient sharply changes. The second is the stable stage, which involves the relatively smooth fluctuation of the friction coefficient mainly because the roughness of the sample surface is much higher, the contact area between the sample and ball is smaller, and the adherent point is relatively rugged in the wear and friction process. As the wear and friction proceeded, the roughness of the material surface was reduced and the convex peak gradually wore off. Thus, the friction coefficient is relatively constant at the stable stage. Compared with the three other kinds of materials, the fluctuation of the friction coefficient of the ZnO-coated whisker reinforced composite is the minimal and its friction coefficient is the maximum (Fig. 2(e)), whereas the friction coefficients of the other three materials are slightly different. The ZnO layer has effectively improved the wettability between the aluminum matrix and the whiskers, resulting in a more uniform and compact composite [14].

Figure 2(f) shows the wear rates of the four materials under the same conditions. It can be seen that the wear rates of the ZnO/$Mg_2B_2O_{5w}$/6061Al, CuO/$Mg_2B_2O_{5w}$/6061Al, $Mg_2B_2O_{5w}$/6061Al and the matrix alloy successively increase, and the wear rate of the ZnO/$Mg_2B_2O_{5w}$/6061Al is almost half that of the matrix alloy. The addition of the whiskers improves the friction and wear properties of the composites, particularly those of the ZnO/$Mg_2B_2O_{5w}$/6061Al and CuO/$Mg_2B_2O_{5w}$/6061Al. On one hand, the friction affects the convex peaks, which is formed by a large number of whiskers during the friction process of the composites. These convex peaks absorb part of the load and the friction, resulting in less contact between the aluminum matrix and the balls, thereby protecting the matrix and reducing the wear rates of the composites. On the other hand, during friction and wear, the whiskers are broken to allow a mechanically mixed layer to form under the pressure in the squeeze. These layers of materials reduce the wear rates of the composites and effectively improve their wear resistance.

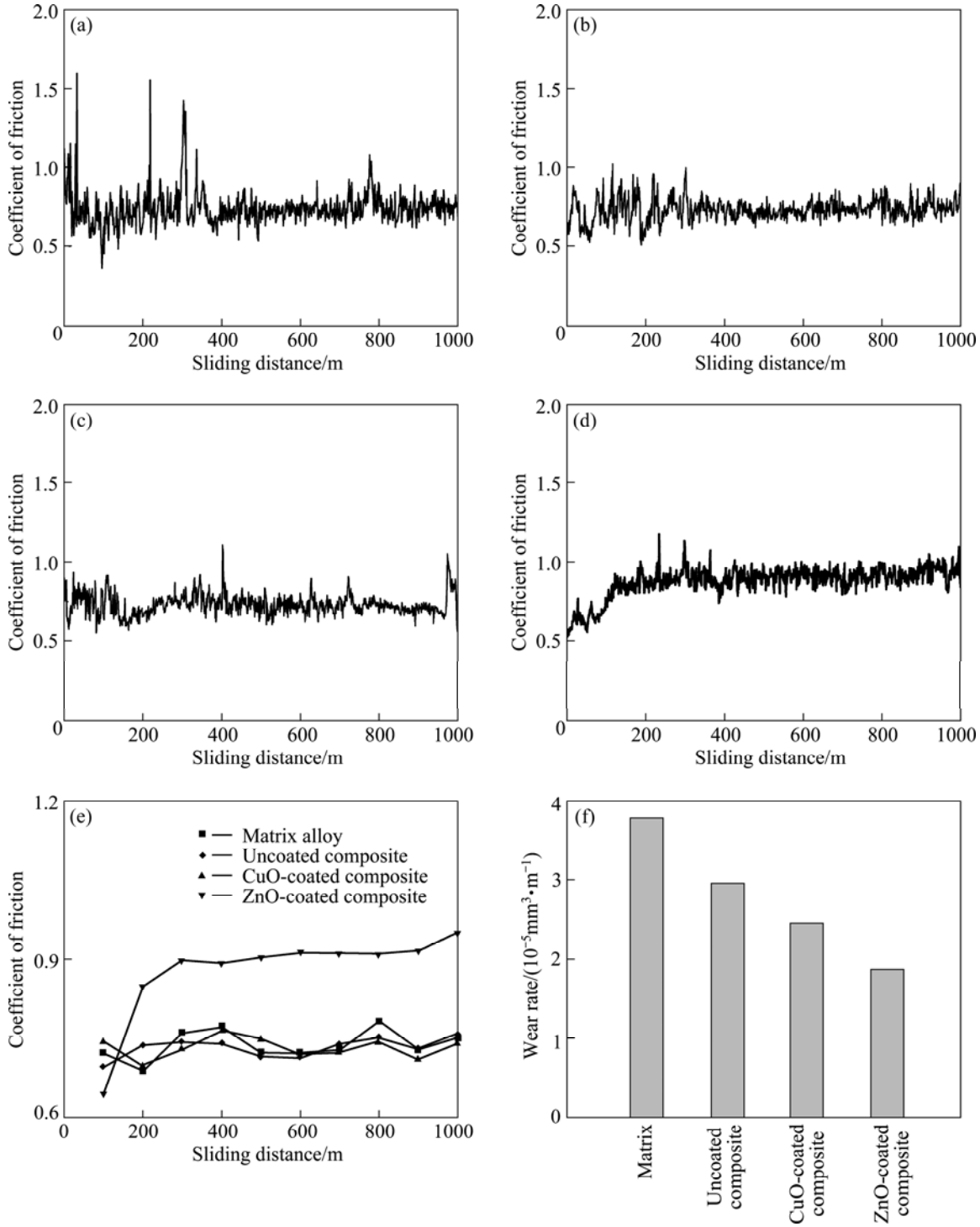

Fig. 2 Wear coefficient (a−e) and wear rate (f) of four materials: (a) Matrix alloy; (b) $Mg_2B_2O_{5w}$/6061Al; (c) CuO/$Mg_2B_2O_{5w}$/6061Al; (d) ZnO/$Mg_2B_2O_{5w}$/6061Al; (e) Comparison of wear coefficients of four materials; (f) Comparison of wear rates of four materials (sliding velocity: 480 m/min; applied load: 15 N)

3.2 Effect of varied applied loads on wear behaviors of composites

Figures 3(a)−(d) show that the friction coefficients of the matrix and composites are gradually reduced and continue to remain stable with increasing sliding distance and sliding time. In all experiments, the friction coefficients become smaller with the increase in the applied loads. These results are in good agreement with those of previous studies [15,16]. At the higher applied loads, the stability of the friction coefficient of the matrix is much higher than that of the composites because of the increase in the roughness of the composite surface. As the experiments proceed, a number of hard convex peaks and grooves caused by abrasive wear are formed on the

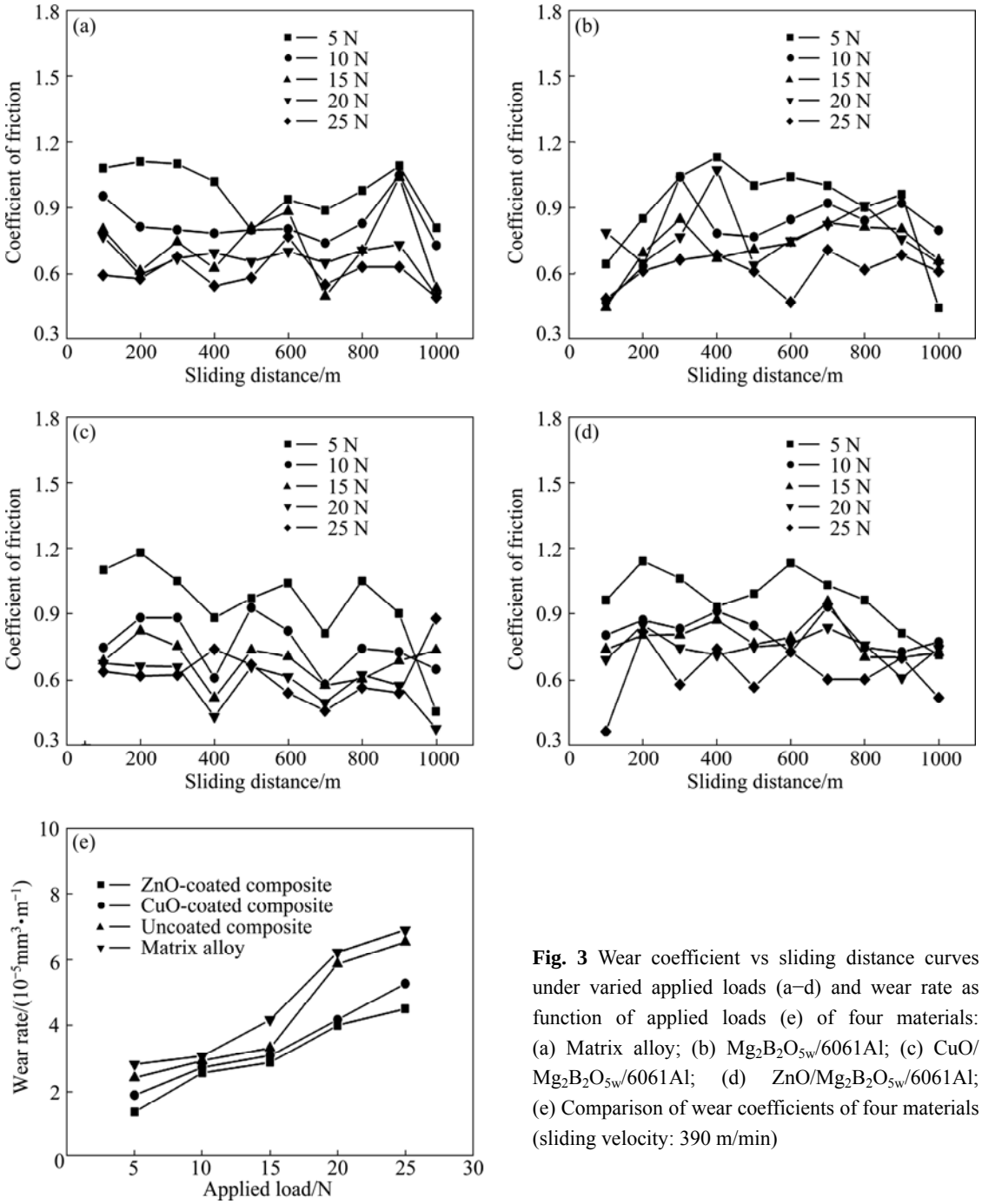

Fig. 3 Wear coefficient vs sliding distance curves under varied applied loads (a−d) and wear rate as function of applied loads (e) of four materials: (a) Matrix alloy; (b) $Mg_2B_2O_{5w}$/6061Al; (c) CuO/$Mg_2B_2O_{5w}$/6061Al; (d) ZnO/$Mg_2B_2O_{5w}$/6061Al; (e) Comparison of wear coefficients of four materials (sliding velocity: 390 m/min)

worn surface. These peaks and grooves cause the sagging and cresting of the worn surface, which results in a significant fluctuation of the friction coefficient. In addition, the temperature can rise with increasing applied load, resulting in the softening of the worn surface and subsurface of the composites and causing significant changes. All these factors can reduce the friction coefficients of the matrix and the composites.

3.3 Effect of varied sliding velocities on wear behaviors of composites

Figure 4 shows the wear coefficients and wear rates of the four materials as a function of the sliding velocities at 15 N. It can be seen that the friction coefficient of the matrix decreases regardless of the sliding velocities. When the sliding velocity reaches 210 m/min, the friction coefficient of the $Mg_2B_2O_{5w}$/6061Al composite is noticeably higher compared with the other three materials. However, when the sliding velocity is above 210 m/min, the friction coefficient of the ZnO/$Mg_2B_2O_{5w}$/6061Al composite is obviously higher compared with the other three materials. This behavior can be attributed to the wettability between the aluminum and the whiskers due to the whisker coated

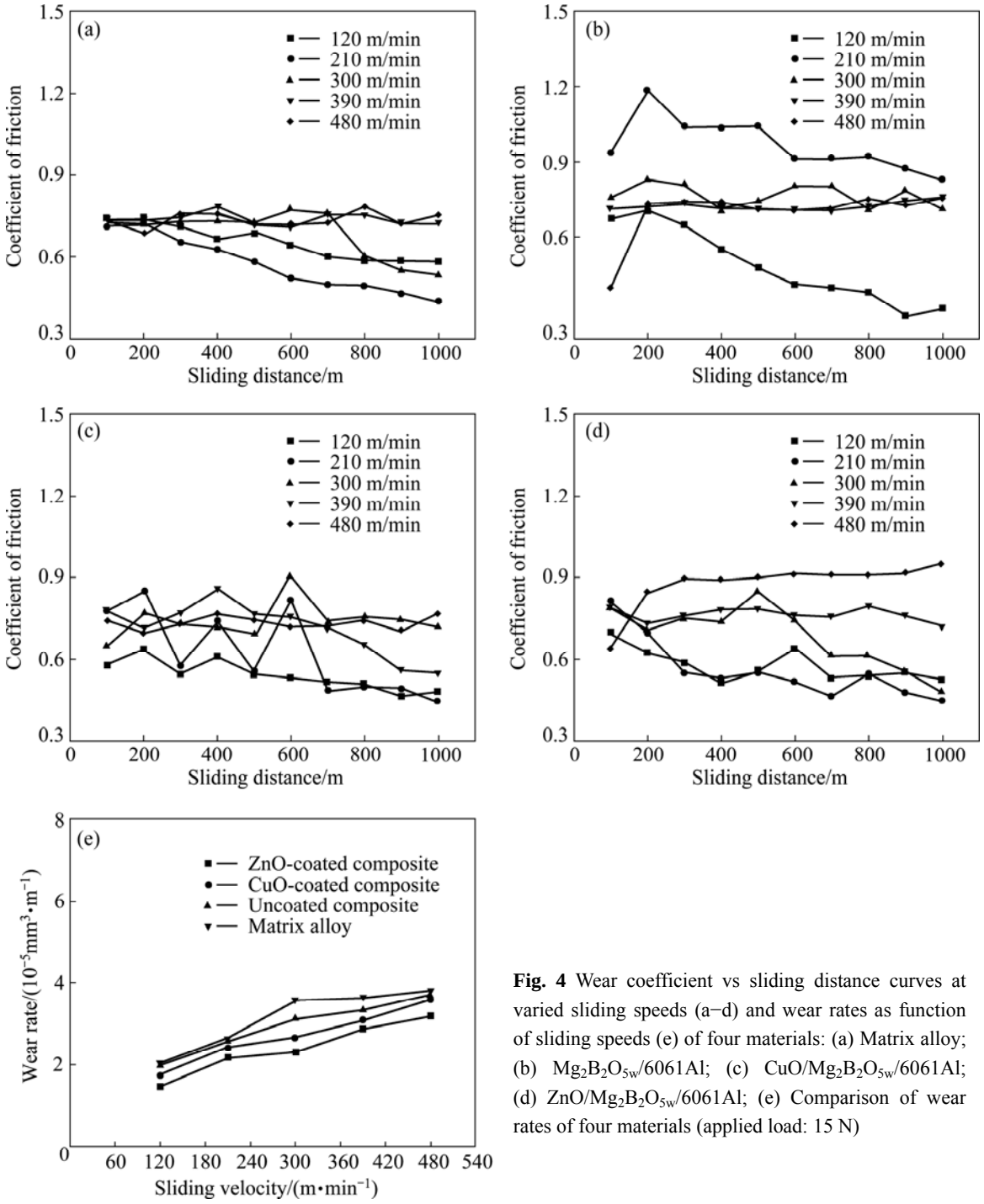

Fig. 4 Wear coefficient vs sliding distance curves at varied sliding speeds (a−d) and wear rates as function of sliding speeds (e) of four materials: (a) Matrix alloy; (b) $Mg_2B_2O_{5w}$/6061Al; (c) CuO/$Mg_2B_2O_{5w}$/6061Al; (d) ZnO/$Mg_2B_2O_{5w}$/6061Al; (e) Comparison of wear rates of four materials (applied load: 15 N)

with ZnO. When the sliding velocity decreases (120 m/min), the effect of the whiskers on the wear rates of the materials becomes negligible, and the wear rates between the matrix and the composites show little variation. The difference of the wear rates between the matrix and the composites is larger with the increase of the sliding velocity from 120 to 300 m/min. Nevertheless, as the sliding velocity further increases from 300 to 480 m/min, the difference of the wear rates between the matrix and the composites gradually decreases.

3.4 Wear morphology

Figure 5 shows SEM images of the worn surface of the matrix alloy at 5 and 25 N and sliding velocities of 120 and 480 m/min, respectively. Figure 5(a) shows that the worn surface appears smooth, with mild wear characteristics and a shallow plough. Figures 5(b)−(d) show that the worn surfaces of the matrices have a large number of deep and long ploughs, cracks (mark *A*), and small cavities (mark *B*).

Figure 6 shows SEM images of the worn surface of

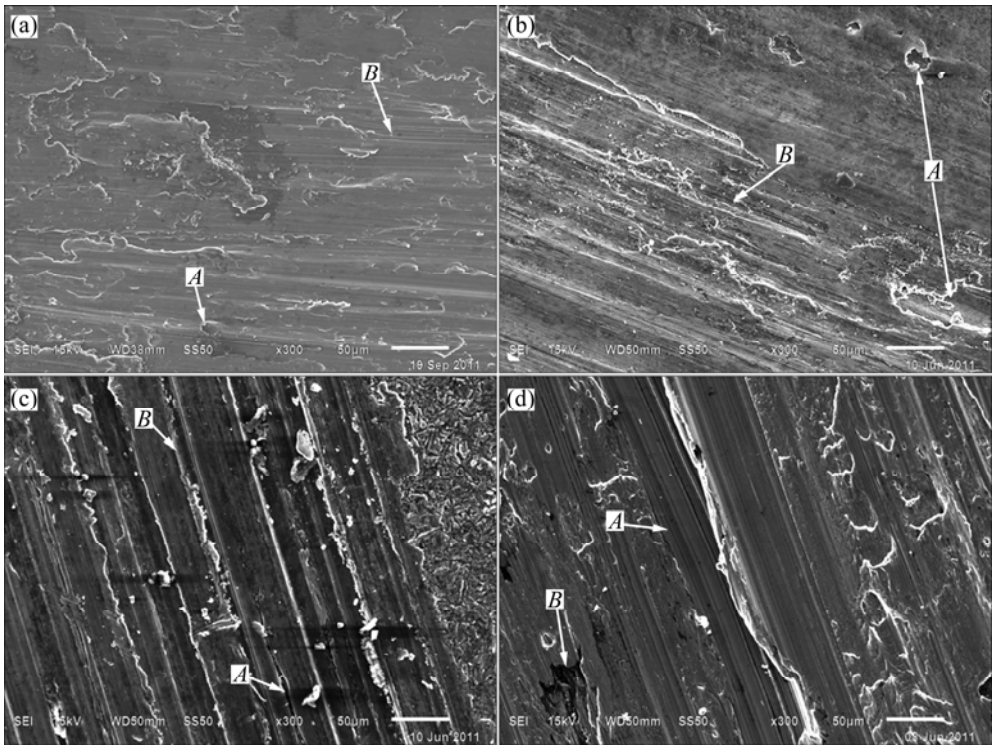

Fig. 5 SEM images of worn surface of matrix alloy under different loads and sliding velocities: (a) 5 N, 120 m/min; (b) 5 N, 480 m/min; (c) 25 N, 120 m/min; (d) 25 N, 480 m/min

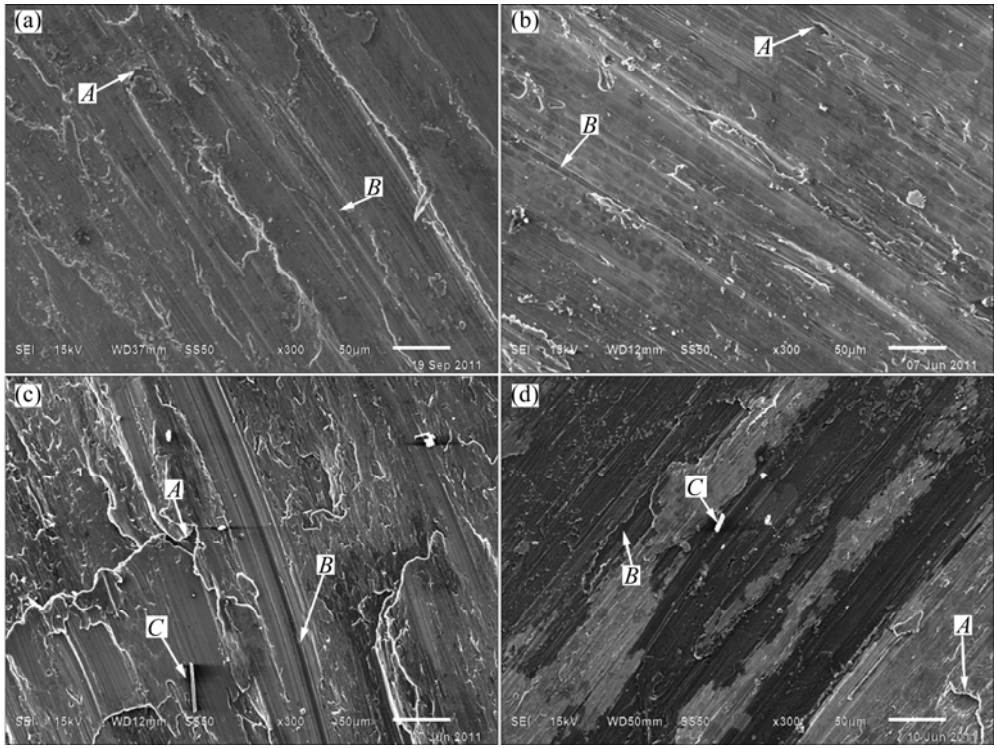

Fig. 6 SEM images of worn surfaces of ZnO/$Mg_2B_2O_{5w}$/6061Al composites under different loads and sliding velocities: (a) 5 N, 120 m/min; (b) 5 N, 480 m/min; (c) 25 N, 120 m/min; (d) 25 N, 480 m/min

the ZnO/$Mg_2B_2O_{5w}$/6061Al composites at 5 and 25 N and sliding velocities of 120 and 480 m/min, respectively. Figure 6(a) shows that the worn surfaces of the composites only show slight cracks and a few small grooves. The large number of whiskers in the composites result in the formation of convex peaks during the friction process of the composite materials. These convex peaks assume part of the load and friction, resulting in less contact between the aluminum matrix and the balls. Figures 6(b)−(d) show that the worn surfaces of ZnO/

$Mg_2B_2O_{5w}$/6061Al composites have a large number of deep and long grooves, cracks (mark *A*), and small holes (mark *B*).

Figure 7(a) shows the morphology of the worn debris at the load of 5 N and a sliding velocity of 120 m/min. The worn debris consists of small granules, and the worn scars are thick and big, indicating a very serious adhesion effect of the aluminum alloy on the grinding ball. The material affected by the mutual friction is the aluminum alloy at the anaphase of the

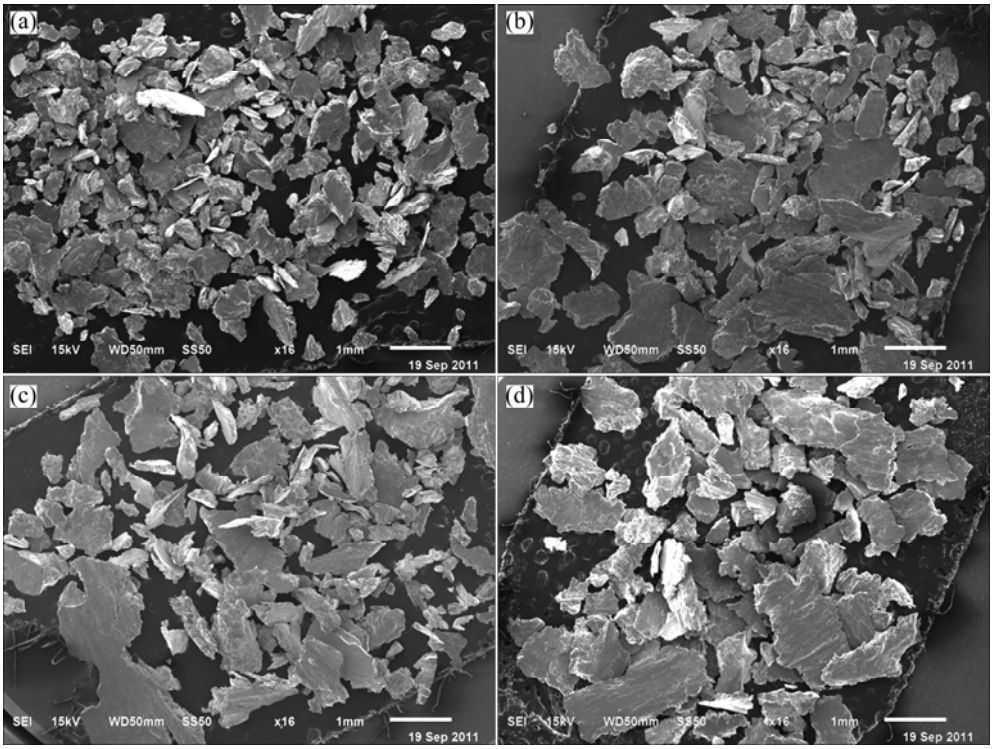

Fig. 7 SEM images showing worn debris morphologies of matrix alloy under different loads and sliding velocities: (a) 5 N, 120 m/min; (b) 5 N, 480 m/min; (c) 25 N, 120 m/min; (d) 25 N, 480 m/min

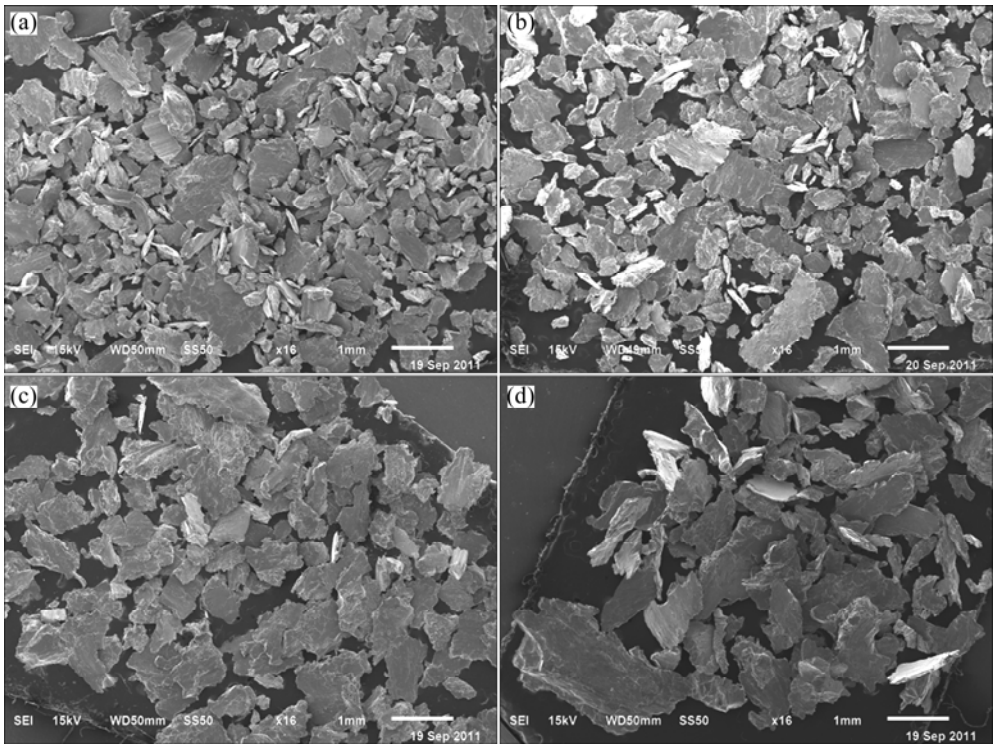

Fig. 8 SEM images showing worn debris morphologies of ZnO/$Mg_2B_2O_{5w}$/6061Al composite under different loads and sliding velocities: (a) 5 N, 120 m/min; (b) 5 N, 480 m/min; (c) 25 N, 120 m/min; (d) 25 N, 480 m/min

wear, and the friction process and wear rate are reduced. At this point, the dominant wear mechanism is adhesive wear, accompanied by mild abrasive wear. With the increase in the sliding velocity and load, the degree of surface that is worn gradually increases due to matrix damage, and the plough of the composites increases and changes from shallow to deep. In addition, the worn surface exhibits a small number of cracks (mark *A*) and cavities (mark *B*) caused by split wear (Figs. 5 and 7).

It was observed from Figs. 7 and 8 that the worn debris of the matrix and ZnO/$Mg_2B_2O_{5w}$/6061Al composite consists of small strips and flakes. The chip size is clearly increased, as well as the number of large flake debris. At the same time, the adhesion of the aluminum alloy on the grinding ball is decreased. The increase in the shear stress between the surfaces results in the transition from adhesive wear to abrasive wear. Increasing the load or the sliding velocity to 25 N and 480 m/min, respectively, significantly increases the surface that is worn. A large number of holes and adhesive tears (mark *B*) are also observed in Fig. 6(d), indicating the occurrence of stripper wear. In addition, a small number of grooves are produced during mild abrasive wear. Compared with Figs. 7(a) and (c), the size (>2 mm) of the debris is significant and, at this condition, the amount of adhesive matrix is reduced to a minimum value. This is due to the high velocity and high load, which causes the worn surface between the samples and the balls to generate a large shear stress that is greater than the shear resistance of the matrix alloy. In turn, this stress results in the formation of a worn surface crack extending along the rubbing direction and forming a large patch of abrasive dust, and the aluminum alloy adheres to the surface of the grinding ball through continuous generation and shedding via the polishing process. These results suggest that this process is not only conducive to the formation of larger debris, but it can also significantly reduce the probability that the matrix alloy will adhere to the grinding ball. The dominant wear mechanism of the matrix is stripper wear, supplemented by a slight abrasive wear.

4 Conclusions

1) The friction and wear properties of the composites appear slight difference for the different types of $Mg_2B_2O_5$ whiskers under similar conditions. The wear rates of the matrix alloys, $Mg_2B_2O_{5w}$/6061Al, ZnO/$Mg_2B_2O_{5w}$/6061Al and CuO/$Mg_2B_2O_{5w}$/6061Al are reduced successively.

2) Under a dry friction condition, the coefficients of friction of the composites tend to be smaller, and the wear rates increase with increasing load or sliding velocity. The wear mechanisms gradually shift from adhesive wear at lower loads or lower velocities to abrasive and delamination wear at higher velocities or higher loads. This shift is associated with microfatigue wear during the friction and wear process. Thus, three kinds of wear simultaneously occur and alternate with one other.

3) SEM analyses of the worn surface of the composites, wear debris, and morphology of the friction surfaces indicate that a large number of grooves, cracks, and holes appear on the worn surface with increasing load. Typical mechanically mixed layers also appear on the grinding surface. Worn debris gradually transforms from small granules to thick sheets, and the adhesive material in the area tends to be less.

References

[1] HIROAKE N, KENJIE K, AKINORI N. Development of aluminum metal matrix composites (Al-MMC) brake rotor and pad [J]. JSAE Review, 2002, 23(3): 365−370.

[2] TANG Bin-bin, JIN Pei-peng, FEI Wei-dong. Flow stress behavior of $Mg_2B_2O_5$w/6061Al composite under hot compression deformation [J]. Transactions of Materials and Heat Treatment, 2012, 33(Sup. II): 7−10.

[3] ANASYIDA A S, DAUD A R, GHAZALI M J. Dry sliding wear behaviour of Al−12Si−4Mg alloy with cerium addition [J]. Materials and Design, 2010, 31(1): 365−374.

[4] MOUSAVI ABARGHOUIE S M R, SEYED REIHANI S M. Investigation of friction and wear behaviors of 2024 Al and 2024 Al/SiCp composite at elevated temperatures [J]. Journal of Alloys and Compounds, 2010, 501(2): 326−332.

[5] WANG You, YANG Yong, ZHAO Yue, TIAN Wei, BIAN Han-min, HE Jun-qi. Sliding wear behaviors of in situ alumina/aluminum titanate ceramic composites [J]. Wear, 2009, 266(11−12): 1051−1057.

[6] JHA N, BADKAL A, MONDAL D P, DAS S, SINGH M. Sliding wear behaviour of aluminum syntactic foam: A comparison with Al−10wt%SiC composites [J]. Tribology International, 2011, 44(3): 220−231.

[7] MINDIVAN H. Reciprocal sliding wear behaviour of B_4C particulate reinforced aluminum alloy composites [J]. Materials Letters, 2010, 64(3): 405−407.

[8] FEYZULLAHOĞLU E, ŞAKIROĞLU N. The wear of aluminium-based journal bearing materials under lubrication [J]. Materials and Design, 2010, 31(5): 2532−2539.

[9] DAOUD A, ABOU EL-KHAIR M T. Wear and friction behavior of sand cast brake rotor made of A359−20 vol% SiC particle composites sliding against automobile friction material [J]. Tribology International, 2010, 43(3): 544−553

[10] TANG Feng, WU Xiao-ling, GE Shi-rong, YE Ji-chun, ZHU Hua, HAGIWARA M, SCHOENUNG J M. Dry sliding friction and wear properties of B_4C particulate reinforced Al-5083 matrix composites [J]. Wear, 2008, 264: 555−561.

[11] BAKSHI S R, WANG D, PRICE T, ZHANG D, KESHRI A K, CHEN Y, McCARTNEY D G, SHIPWAY O H, AGARWAL A. Microstructure and wear properties of aluminum/aluminum-silicon composite coatings prepared by cold spraying [J]. Surface and Coatings Technology, 2009, 204 (3): 503−510.

[12] MOUSAVI ABARGHOUIE S M R, SEYED REIHANI S M. Investigation of the friction and wear behaviors of 2024 Al alloy and 2024 Al alloy/SiCp composite at elevated temperatures [J]. Journal of Alloys and Compounds, 2010, 501: 326−332.

[13] JIN Pei-peng, HAN Li, CHEN Shan-hua, WANG Jin-hui, ZHU

Yun-peng. Microstructure and tensile properties of ZnO-coated magnesium borate whisker reinforced AZ31B composite [J]. Materials Science and Engineering A, 2012, 554(6): 48−52.

[14] FEI W D, JIANG X D, LI C. Effect of interfacial reaction on the fracture behavior of alumina borate whisker reinforced aluminium composite [J]. Materials Science and Technology, 1997, 13(11): 918−922.

[15] MONDAL D P, DAS S, JHA N. Dry sliding wear behavior of aluminum syntactic foam [J]. International Journal of Materials and Design, 2009, 30: 2563−2568.

[16] RAO R N, DAS S. Wear coefficient and reliability of sliding wear test procedure for high strength aluminium alloy and composite [J]. International Journal of Materials and Design, 2010, 31(7): 3227−3233.

硼酸镁晶须增强 6061 铝基复合材料的干摩擦磨损行为

金培鹏，陈 庚，韩 丽，王金辉

青海大学 机械工程学院，西宁 810016

摘 要：研究搅拌铸造工艺制备的硼酸镁晶须增强 6061 铝基复合材料在干滑动条件下的摩擦磨损性能。复合材料的体积分数为 2%，根据增强体种类，材料分别记为：Al 基体、$Mg_2B_2O_5$w/6061Al、ZnO/$Mg_2B_2O_5$w/6061Al 和 CuO/$Mg_2B_2O_5$w/6061Al；讨论磨损速率和摩擦因数之间的关系。结果表明：在 4 种材料中，ZnO/$Mg_2B_2O_5$w/6061Al 复合材料的磨损率最低。随着载荷和滑动速度的增大，基体和复合材料的摩擦因数和磨损率降低，摩擦磨损机制由轻微磨损机制转向严重磨损机制。

关键词：金属基复合材料；滑动磨损；磨损试验；磨损机制

(Edited by Xiang-qun LI)